PRAMANA
— journal of
physics

Vol. 42, No. 2,
February 1994
pp. 107–122

Leptodermous expansion of nuclear ground state energies and the anomaly in the nuclear curvature energy

S K KATARIA[1], ARUNA NIJASURE[1], V S RAMAMURTHY[2] and A K DUTTA[3]
[1]Bhabha Atomic Research Centre, Bombay 400085, India
[2]Institute of Physics, Bhubaneshwar 751005, India
[3]Department of Physics, D.A. University, Indore 452001, India

MS received 7 December 1992; revised 2 November 1993

Abstract. The leptodermous expansion of the total ground state energy of a nucleus into volume, surface, curvature and gauss curvature contributions has been studied starting from a semi-classical energy density formalism of extended Thomas Fermi type. A numerical procedure was used to obtain the surface energy and curvature energy contributions from surface moments of energy density profiles $H(r)$ for a sequence of nuclei with $N = Z$ and neglecting the coulomb interaction for the three Skyrme forces. A transition to the liquid drop model type expansion in increasing powers of $A^{-1/3}$ is then made, taking into account the dependence of the central density and the surface structure on the mass of the nucleus. It is found that there is no inconsistency between the curvature contribution to the total energy in the leptodermous expansion and the $A^{-1/3}$ term contribution in the liquid drop model expansion. It has been shown that the earlier apparent anomaly between the above two methods arises due to the use of semi-infinite approximation and the mass dependence of the central density and the surface structure of finite nuclei.

Keywords. Leptodermous expansion; liquid drop model; surface energy; curvature energy; finite nuclei; extended Thomas Fermi calculations; Euler's equations.

PACS No. 21·10

1. Introduction

The concepts of leptodermous system have been extensively discussed in several review articles [1]. Due to the short range of the nuclear forces, the thickness of nuclear surface a is rather small compared to the nuclear radius R except for the very light ones. The ratio a/R can then be used as an expansion parameter in a power series expansion of various quantities in a nucleus such as their ground state energy per nucleon in increasing power of a/R. Such a leptodermous expansion [2] leads to a decomposition of the total ground state energy of a finite nucleus into volume, surface, curvature and Gauss curvature contributions. It is also well-known that nuclear radii exhibit approximately an $A^{+1/3}$ dependence arising from the saturation property of nuclear forces and consequently near constancy of the central density for all the nuclei. This makes it possible to expand several nuclear properties in increasing powers of $A^{-1/3}$. This liquid drop model expansion forms the basis of all semi-empirical mass formulae used to fit experimental ground state masses and fission barriers. While it is customary to associate the leading terms of the liquid drop model expansion a volume, surface and curvature interpretation, this could only be

approximate, since the nuclear fluid is not strictly incompressible. Recently, an apparent anomaly has been noticed between the nuclear curvature energies in a leptodermous expansion and the $A^{+1/3}$ term in a liquid drop model expansion of the nuclear ground state energies. Myers and Swiatecki [3] have observed that in the framework of the droplet model best fits to the experimental ground state masses are obtained when the coefficient of the $A^{+1/3}$ term is assumed to be zero. In another study, Seegar and Howard [4] obtained a value of $-0{\cdot}76 \pm 0{\cdot}11$ MeV for the coefficient of the $A^{+1/3}$ term. In the folding model of Krappe *et al* [5], for the surface energy, the curvature energy turns out to be identically zero. On the other hand, leptodermous expansions of the nuclear ground state energies have always yielded much higher values of the nuclear curvature energies, corresponding coefficients of the $A^{+1/3}$ term ranging from 9–15 MeV [6]. Negele and Vautherin [7] using Hartree Fock calculations with Skyrme interactions for a sequence of mirror nuclei without Coulomb interaction obtained the value of curvature contribution as 11·86 MeV. In many recent studies it has been concluded that this anomaly cannot be resolved within the framework of the existing calculations of the ground state energies [8].

In the present work, we have studied in detail leptodermous expansion of the nuclear ground state energies starting [9] from a suitably chosen semiclassical energy density functional. A transition is then made to a liquid drop model expansion taking into account the dependence of the central density, surface diffuseness and surface skewness on the mass number of the nucleus. It is shown that there exists no anomaly between the calculated curvature energies and the coefficient of the $A^{+1/3}$ term in the LDM expansion, if the transition from the leptodermous expansion to the LDM expansion is carried out properly. Previous calculations [1, 6, 8, 10] of curvature contribution have been carried out for semi-infinite surfaces as these only can be carried out analytically. Calculations of curvature energies with semi-infinite model surfaces miss important physical features and result in misleading conclusions.

2. Leptodermous and LDM expansions of nuclear ground state energies

In the framework of energy density formalism [11], the total energy of a nucleus can be written as a volume integral of a suitably chosen energy density $H(r)$

$$E_T = 4\pi \int_0^\infty H(r) r^2 \mathrm{d}r \tag{1}$$

where $H(r)$ is a functional of the density $\rho(\mathbf{r})$ and its derivatives. In the present analysis, we restrict ourselves to the case of spherical nuclei with $N = Z$ and without Coulomb interaction. For leptodermous nuclei, the contribution from the surface region to the total energy can be isolated by expanding E_T in terms of the surface moments of $H(r)$ around the nuclear sharp-cutoff radius R_s, defined by the relation:

$$A = 4\pi/3 R_s^3 \rho_0 \tag{2}$$

where central density of a nucleus is denoted by ρ_0 and A is its mass number. For calculation of surface moments around R_s, we substitute $r = R_s + z$ in (1), and obtain

$$\begin{aligned} E_T &= 4\pi \int_{-R_s}^\infty H(z + R_s)(R_s + z)^2 \mathrm{d}z \\ &= 4\pi \left[\int_{-R_s}^0 H(z + R_s)(R_s + z)^2 \mathrm{d}z + \int_0^\infty H(z + R_s)(R_s + z)^2 \mathrm{d}z \right]. \end{aligned}$$

Rewriting the first integral as

$$4\pi \int_{-R_s}^{0} [H(z+R_s) - \varepsilon_0 + \varepsilon_0](R_s+z)^2 \mathrm{d}z$$

where ε_0 is the central energy density corresponding to the density ρ_0, one has

$$E_T = \varepsilon_0 \frac{4\pi}{3} R_s^3 + 4\pi \int_{-R_s}^{0} [H(z+R_s) - \varepsilon_0](R_s+z)^2 \mathrm{d}z + 4\pi \int_0^{\infty} H(z+R_s)(R_s+z)^2 \mathrm{d}z$$

and expanding the $(R_s+z)^2$ terms in the integrals, we have

$$\begin{aligned} E_T &= \varepsilon_0 V + S\left[\int_{-R_s}^{0} [H(z+R_s) - \varepsilon_0]\mathrm{d}z + \int_0^{\infty} H(z+R_s)\mathrm{d}z\right] \\ &\quad + 4\pi R_s\left[\int_{-R_s}^{0} [H(z+R_s) - \varepsilon_0]z\mathrm{d}z + \int_0^{\infty} H(z+R_s)z\mathrm{d}z\right] \\ &\quad + 4\pi\left[\int_{-R_s}^{0} [H(z+R_s) - \varepsilon_0]z^2\mathrm{d}z + \int_0^{\infty} H(z+R_s)z^2\mathrm{d}z\right] \\ &= a_v V + a_s S + a_c C + a_G G; \quad \text{where } G = 4\pi \text{ and } C = 4\pi R_s \end{aligned} \tag{3}$$

where V is the volume of the nucleus with sharp cutoff radius R_s, S is its surface area, C is its mean radius of curvature and G is its Gaussian curvature. Because of the asymptotic constancy of the energy density $\varepsilon(r)$ for $r \ll R_s$, integrands in all the three terms are sharply peaked around R_s with a range of the order of diffuseness parameter a. The first term in this leptodermous expansion can be identified as the volume energy of the nucleus, the second term its surface energy, the third term its curvature energy and the fourth term corresponds to the Gaussian curvature energy.

In principle, the above expansion could have been carried out around any expansion radius R, e.g. in place of the sharp cut-off radius by half density radius $R_{1/2}$ [10]. To this extent, the decomposition of the total energy into volume and surface contributions is not unique but depends on the choice of the expansion radius. In case expansion is carried out around $R_{1/2}$, the first term will not be proportional to mass number A but will also involve additional contributions of the order of a/R. A similar expansion of the density profile $\rho(r)$ around half density radius $R_{1/2}$ gives the relation between the mass number A and $R_{1/2}$ involving these $a/R_{1/2}$ correction terms in terms of various surface moments of $\rho(r)$ as in eq. (3) for energy density profiles. Hence, for the surface moments of the energy density profiles calculated around this radius, one will have to invert the leptodermous expansion of the density profiles in order to make the transition to the LDM type expansion in $A^{-1/3}$. However, in the present studies, with the choice of expansion radius as the sharp cut-off radius R_s, the volume energy turns out to be proportional to particle number A, which is an advantage in a subsequent transition to liquid drop model expansion. Hence our choice of R_s as the expansion radius. This choice is also consistent with the earlier analysis [6] of surface and curvature energies with model semi-infinite surfaces.

If the nuclear fluid had been incompressible, a transition to the LDM expansion

is trivial since

$$R_s = (3A/4\pi\rho_0)^{1/3}$$

and

$$E_T = a_v^* A + a_s^* A^{2/3} + a_c^* A^{1/3} + a_G^* \tag{4}$$

The LDM coefficients a_v^*, a_s^*, a_c^* and a_G^* are uniquely related one-to-one to the leptodermous expansion coefficients a_v, a_s, a_c and a_G. However, the nuclear fluid is compressible with a finite compressibility coefficient. The central density and the structure of the nuclear surface, namely, its thickness and skewness are then dependent on the mass number A of the nucleus. Therefore, the coefficients a_v, a_s, a_c and a_G in (3), are not universal constants but depend on the mass number A. For example, the central density of finite nuclei using semi-classical energy density formalism has been studied in detail earlier [1]. Defining the parameter ε as

$$\varepsilon = -1/3\ (\rho_0 - \rho_\infty)/\rho_\infty \tag{5}$$

where ρ_∞ is the saturation density of nuclear matter. The leptodermous expansion coefficients for the total energy of the nucleus were expanded as

$$\begin{aligned} a_v &= a_v^\infty + 1/2\ K_\infty \varepsilon^2 - 9/2\ \ddot{a}_v \varepsilon^3 \\ a_s &= a_s^\infty - 3\dot{a}_s \varepsilon + 9/2\ \ddot{a}_s \varepsilon^2 \\ a_c &= a_c^\infty - 3\dot{a}_c \varepsilon + 9/2\ \ddot{a}_c \varepsilon^2 \end{aligned} \tag{6}$$

where dots denote the derivatives with respect to ρ_0; a_v^∞, a_s^∞ and a_c^∞ are the nuclear matter values and K_∞ is the corresponding incompressibility. To the lowest order, the mass dependence of ε can be written as (similar to droplet model)

$$\varepsilon = 3\dot{a}_s A^{-1/3}/K_\infty = -2a_s^\infty A^{-1/3}/K_\infty. \tag{7}$$

It is, therefore, reasonable to express the leptodermous expansion coefficients for finite nuclei as:

$$\begin{aligned} a_v &= a_v^\infty + a_v'' A^{-2/3} + a_v''' A^{-1} \\ a_s &= a_s^\infty + a_s' A^{-1/3} + a_s'' A^{-2/3} \\ a_c &= a_c^\infty + a_c' A^{-1/3} \\ a_0 &= a_0^\infty \end{aligned} \tag{8}$$

where we have used the dashes denoting the derivatives with respect to $A^{-1/3}$, and a_v^∞, a_s^∞ and a_c^∞ are the nuclear matter values. In addition to the variations of the central density with mass number, there could also be mass variations of the surface structure (diffuseness and skewness) for finite nuclei [6] and have not been studied in detail. However, one could use expansions of the type given by the eq. (8) in general. The nuclear matter values for the volume and surface contributions can be evaluated by taking the limit $A^{-1/3} \to 0$. The other coefficients are not of simple nature and are to be evaluated numerically only. A transition to the LDM then implies that the coefficients a_c^* and a_G^* have contributions from lower order terms. For example, the

coefficient of $A^{+1/3}$ in (4) has, in addition, to the curvature contribution, has also components from surface and volume terms as given in (8)

$$a_c^* = a_c^\infty + a_s' + a_v''. \tag{9}$$

For a quantitative study of the decomposition of a_c^*, we use the energy density formalism as described below.

3. Numerical studies with semi-classical energy densities

According to the semi-classical energy density formalism any physical quantity can be expressed as a functional of nuclear densities of the two fluids $\rho_q^A(q = n, p)$. The construction of the functional for the total energy requires separate analysis for the kinetic and potential parts. For the kinetic energy part, the second order extended Thomas Fermi Functional involving inhomogeneity corrections up to second order only in the derivatives of the density ρ_q is written as [6]

$$\tau(\rho_q) = \alpha\rho_q^{5/3} + \beta(\nabla\rho)_q^2/\rho_q + \gamma\Delta\rho_q \tag{10}$$

As is well-known, for extended Thomas Fermi (ETF2) functional $\alpha = 3/5(3\pi^2)^{2/3}$ and $\beta = 1/36$ and $\gamma = 1/3$. However, this ETF2 is not a very good approximation at the nuclear surface, where the potential is rapidly varying and one has to go to fourth order corrections in this part. In modified Thomas Fermi (MTF) approach, the nuclear surface properties were shown to be well reproduced [6] using the form given in (10) with $\alpha = 3/5(3\pi^2)^{2/3}$ and $\gamma = 1/3$ and treating β as a free parameter. In the present work, we have used $\beta = 1/18$ and $\beta = 1/36$ for ETF2 calculations.

For the potential part, the use of zero-range Skyrme interaction simplifies the definition of the hamiltonian energy density, which, without any further approximation, depends only on the nuclear density and the kinetic energy density. The Skyrme functional for the total energy density $E(r)$ for a closed shell nuclei with $(\rho_n(r) = \rho_p(r) = 1/2\rho(r))$ can be written as

$$\begin{aligned} E(r) = {} & h^2/2m^*(\mathbf{r})\tau(\mathbf{r}) + 3/8\ t_0\rho^2(\mathbf{r}) + 1/64\ (9t_1 - t_2(5 + 4x_2))(\nabla\rho)^2 \\ & + 1/16\ t_3\rho^{2+\alpha}(\mathbf{r}) + 3/4\ W_0(\mathbf{J}\cdot\nabla\rho) \end{aligned} \tag{11}$$

where the effective mass $m^*(r)$ for the Skyrme forces is given by

$$f(r) = m/m^*(r) = 1 + 1/16[3t_1 + t_2(5 + 4x_2)]\rho(\mathbf{r})$$

and $\mathbf{J}$ is the spin current density,
and t_0, t_1, t_2, t_3, x_2 and W_0 are the parameters of the Skyrme forces. There is a whole series of Skyrme force parametrization labelled SI, SII, SIII, SIV, SkM and RATP giving different set of values to the above constants. It is well known that the surface energy coefficient and curvature energy coefficients depend significantly on the choice of these parameter sets. In our calculations, we have studied the leptodermous expansion for the SIII, SkM and RATP Skyrme parameter sets as given in table 1. The densities $\tau(\mathbf{r})$ and $\mathbf{J}(\mathbf{r})$ are universal functional of the local density [11, 12] and in the semi-classical ETF approach, including the terms arising from the effective mass are

$$\tau(r) = \tau_{TF}(\rho(r)) + \tau_2(\rho(r)) \tag{12}$$

Table 1. Parameters of the Skyrme forces used in the present work from refs [1,6].

Force	t_0 MeVfm^3	t_1 MeVfm^5	t_2 MeVfm^5	t_3 MeVfm$^{3+3\alpha}$	x_0	x_1	x_2	x_3	α	W_0
SIII	−1128·75	395·00	−95	14000	0·45	0·0	0·0	1·0	1	120·00
SkM	−2646·00	385·00	−120	15595	0·09	0·0	0·0	0·0	1/6	130·00
RATP	−2160·00	513·00	+121	11600	0·418	−0·36	−2·29	0·586	1/5	120·00

$$\tau_2(\rho) = 1/36\ (\nabla\rho)^2/\rho + 1/3\ \Delta\rho + 1/6\ \nabla f\cdot\nabla\rho/f + 1/6\ \rho\nabla^2 f/f - 1/12\ \rho(\nabla f/f)^2 + 1/2\ (2m/\hbar^2)^2\rho(W/f)^2 \tag{13}$$

and $\mathbf{J}(\rho) = -2m/\hbar^2\,\rho/f\,\mathbf{W} = -3/2\ W_0 2m/\hbar^2\,\rho/f\nabla\rho$.

The minimization of the total energy E_T, written as a functional $H(\rho)$ of matter density $\rho(r)$ leads to the two coupled Euler's equations

$$\frac{\partial H}{\partial \rho_q} - \nabla\cdot\frac{\partial H}{\partial \nabla\rho_q} + \Delta\frac{\partial H}{\partial \Delta\rho_q} = \lambda_q \quad q = n, p \tag{14}$$

where λ_n and λ_p are Langrange multipliers corresponding to the conservation of the number of neutrons and protons. These Euler's equations are second order differential equations which have been solved numerically in the case of finite systems as well as for semi-infinite systems to obtain the density profiles. The density profile systematics for finite nuclear systems have been studied earlier [6]. In our calculations, we have used the same code to obtain the mass dependence of the nuclear surface structure.

Alternatively, the minimization of E_T can be carried out by assuming some analytical form of the semiclassical density $\rho(r)$ and minimizing it with respect to the density profile parameters. This procedure corresponds to a limited variation in some subspace defined by the analytic form of the density profiles. Generalized Fermi functions as given below

$$\rho(r) = \rho_0/\{1 + \exp(r - R)/a\}^{\nu} \tag{15}$$

have been shown to adequately describe the density profiles for the finite nuclei and are very close to the solutions of the Euler's equation. This method has the advantage of the faster convergence over that of Euler equations [12].

We have calculated the total energy E_T, as well as the three surface moments E_s, E_c and E_0 using the density profiles obtained in two ways: (i) by solving the Euler's equations and, (ii) by method of least squares to obtain the parameters of the modified Fermi distributions for a number of nuclei in the mass range $40 < A < 500$. It was found that the differences in the quantities E_T, E_s, E_c and E_0 in these two ways are of the order of 1–5 MeV (see for example E_T values in columns a and b for cases I and III in table 2), and therefore any of these two methods can be used in calculations.

Figure 1 shows the plot of density profile for a very heavy nucleus $A = 500$ calculated using the first method for the SIII interaction. As seen in figure 1, density $\rho(r)$ can be well represented by a generalized Fermi distribution. The plot of corresponding energy density $H(r)$ is also shown in the figure. One observes that the maximum occurs in the vicinity of the nuclear surface and not at the centre of the nucleus, and

Table 2. Total energy of nuclei calculated with SIII interaction and $\beta = 1/18$.

A	Case I (a)	Case I (b)	Case II (a)	Case III (a)	Case III (b)
500	−6703·0	−6704·6	−6560·9	−6423·5	−6428·1
300	−3879·2	−3880·2	−3777·3	−3642·8	−3647·4
200	−2497·2	−2498·0	−2419·0	−2290·6	−2295·2
140	−1685·3	−1685·9	−1623·4	−1501·8	−1506·6
100	−1156·0	−1156·4	−1106·2	−992·0	−997·0
80	−896·7	−896·5	−853·8	−744·6	−749·2
60	−642·8	−642·3	−607·4	−505·4	−508·7
40	−397·0	−397·4	−369·9	−277·0	−281·3

(a) using density profiles calculated from Euler's equation with total $H(r)$. The total energy is calculated using the same density profile with three prescriptions for $\tau(\rho)$.
Case I with complete ETF-2 and MTF values for β and γ parameters,
Case II, $\Delta\rho = \rho''$ was assumed for $\tau(\rho)$ for the calculation of $H(r)$ keeping $\rho(r)$ as in case I estimate.
Case III, E_T was calculated using $\Delta\rho = 0$ in $\tau(\rho)$ expressions.
(b) Same as (a) but using modified Fermi distributions for $\rho(r)$, whose parameters were obtained by minimising the total energy E_T with and without the Δ-term in the calculation of $H(r)$.

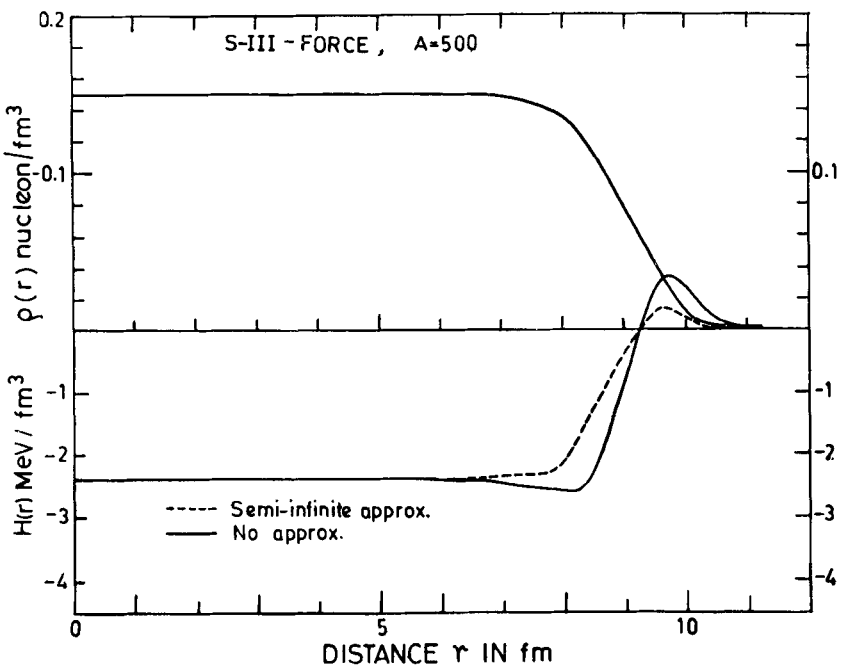

Figure 1. The plots of density distribution $\rho(r)$ and energy density distribution $H(r)$ for $A = 500$, SIII force with $\beta = 1/18$. The continuous curve is for $H(r)$ and dotted curve is obtained by approximating $\Delta\rho = \rho''$ in τ terms and using the same density profile $\rho(r)$ shown in the figure.

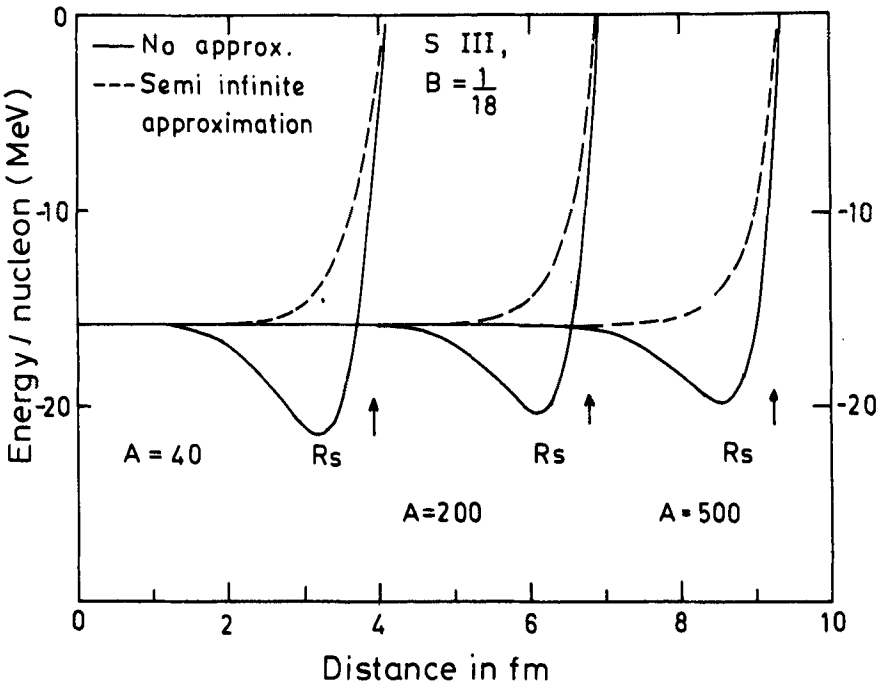

Figure 2. The plot of energy per nucleon $H(r)/\rho(r)$ for $A = 40$, 100 and 500 as a function of r for SIII force as in figure 1. The continuous curve is for total $H(r)$ and dashed curve is obtained under semi-infinite approximation in τ term.

also that the energy density shows positive values outside the sharp cutoff radius. The extra binding energy in the surface region arises due to the Lapalacian term in the kinetic energy term $\tau(r)$, and the contribution of this term increases with decreasing mass number A, due to the presence of $2/r\ \partial/\partial r$ term in the Δ operator. However, the plot of $H(r)$ calculated by approximating $\Delta\rho \simeq \partial^2\rho/\partial r^2$ in its kinetic energy term $\tau(r)$ (termed in this work as semi-infinite approximation) does not show maximum value in the surface region and the positive energy peak is also of much smaller magnitude.

The plots of energy density per nucleon $H(r)/\rho(r)$ as a function of r for three mass numbers $A = 40, 200$ and 500 are shown in figure 2. The surface peaking of the energy density per nucleon is not present when it is calculated in the semi-infinite approximation in the calculation of $H(r)$ and for the same density profiles, shown as dashed curves in figure 2. For the case of smaller nucleus $A = 40$, the maximum in the $H(r)/\rho(r)$ is larger than for the case of very heavy nucleus like $A = 500$. This clearly brings out the dependence of the energy density profiles on the mass number A and also the term responsible for it.

The calculated total energy E_T for a number of nuclei using the density profiles calculated by

(a) solving Euler's equations
(b) the parametrized form given by (15) of $\rho(r)$

are given in table 2 for SIII parameters under different approximations in the kinetic term τ, but using the same density profiles. In this table, case I is for the total energy of the nuclei calculated using τ as given in (10). In case II, E_T is calculated by assuming

that the $\Delta\rho = \partial^2\rho/\partial r^2$ in the terms involving τ. In case III, E_T is calculated by neglecting the $\Delta\rho$ terms in the calculation of τ. As can be seen from table 2, the calculated value of E_T under the three cases are significantly different and arise due to the contribution of terms involving the integral $\int\rho\Delta\rho\,d^3r$, and the relative magnitude of this term increases for smaller nuclei.

In earlier self-consistent calculations i.e. solving Euler's equations exactly [6], it was observed that the effective surface diffuseness related to the (10%–90%) distance is almost independent of mass number, although the parameters (r_0, a, v) of generalized Fermi distribution were found to vary. In order to quantify this mass dependence of nuclear surface structure we have calculated the surface moments of the density profiles around the inflexion point up to fourth order for SkM* force. Figure 3 shows the mass dependence of these surface moments of the density profile, and of the sharp cut-off radius parameter r_0. The skewness parameter μ_3 and μ_4 show large variation with mass number, whereas μ_2 varies rather slowly. The surface tension coefficient is known to depend on the width of the integrand, and therefore, the mass dependence of nuclear surface structure will not alter its estimate significantly. However, the curvature energy, which is the first moment of the surface peaked integrand in (3) and depend on the μ_3 and μ_4 surface moments will show large contribution from

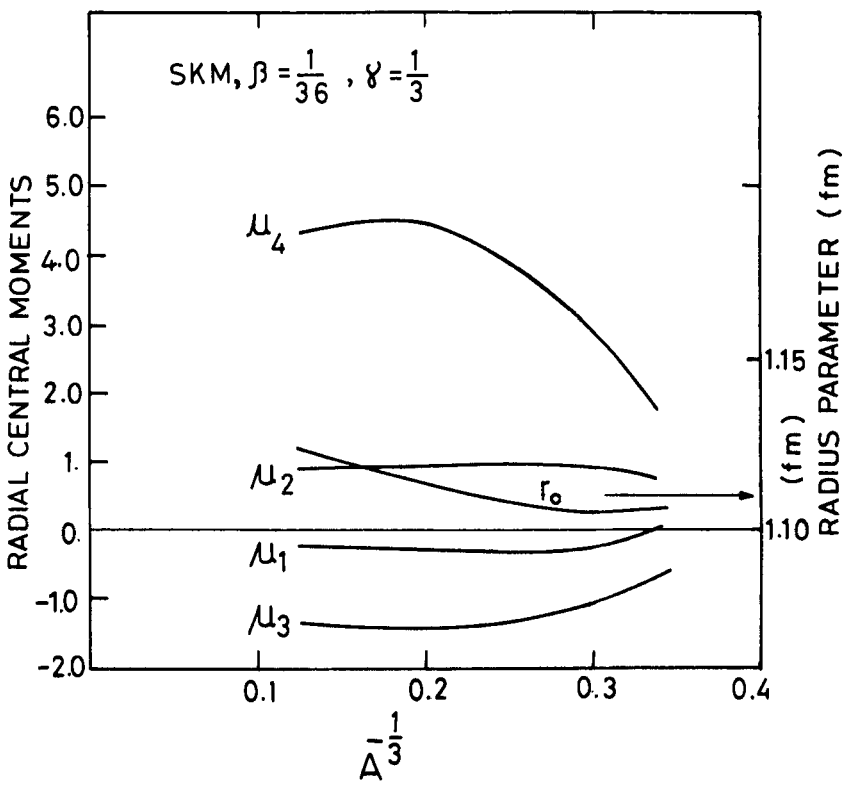

Figure 3. The plot of central moments $\mu_1, \mu_2, \mu_3, \mu_4$ of density distribution $\rho(r)$ around its inflexion point as a function of $A^{-1/3}$. The variation of sharp-cutoff radius parameter r_0 is also shown in the figure.

the mass dependence of the nuclear surface structure. The plot of r_0 as a function of $A^{-1/3}$ shows compressibility effects for larger nuclei $A > 100$ and for smaller masses the compression by the surface tension is compensated by surface structure changes. The magnitude of these quantities are a very sensitive function of the choice of kinetic energy functional and the Skyrme force parameters, but the general trends remain unchanged.

One can also calculate the surface moments of the energy density $H(r)$ for diffuse density distributions [10] $\rho(r)$ as

$$E_T = \varepsilon_0 A + S\left[\int_{-R_s}^{0} [H(\rho(r)) - \varepsilon_0 \rho(r)]\,dz + \int_0^{\infty} H(\rho(r))\,dz\right] + C\left[\int_{-R_s}^{0} [H(\rho(r)) - \varepsilon_0 \rho(r)]z\,dz + \int_0^{\infty} H(\rho(r))z\,dz\right] + G\left[\int_{-R_s}^{0} [H(\rho(r)) - \varepsilon_0 \rho(r)]z^2\,dz + \int_0^{\infty} H(\rho(r))z^2\,dz\right]. \quad (16)$$

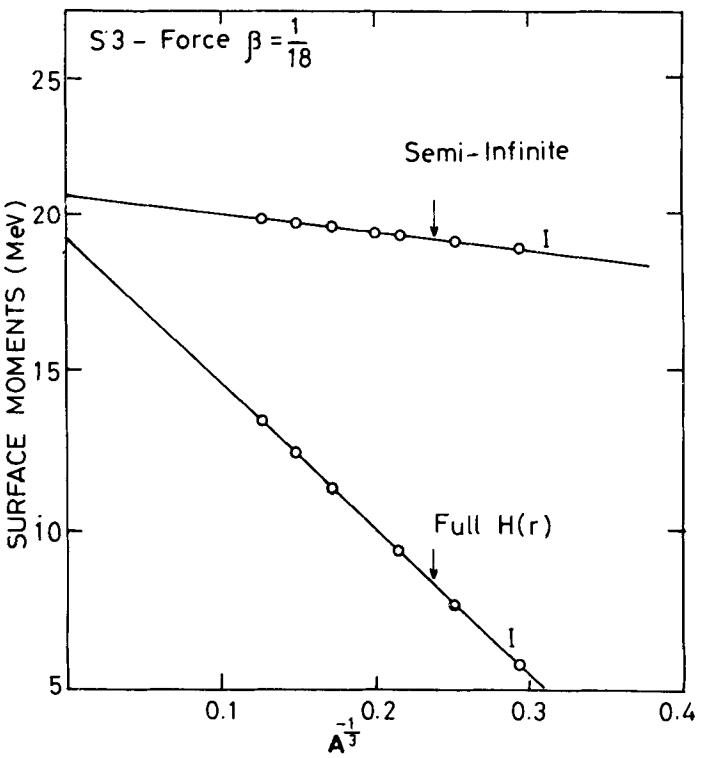

Figure 4. The plot of surface moments of energy density profile $H(r)$ around R_s as a function of $A^{-1/3}$. The semi-infinite values are calculated by $\Delta\rho = \rho''$ approximation in τ-terms.

However, we have calculated the surface moments around sharp cut-off radius using (3) for a number of nuclei and with density profiles calculated in two ways. Figure 4 shows the plot of the surface energy coefficient as a function of $A^{-1/3}$. The extrapolation of these quantities in the nuclear matter limit $A \Rightarrow \infty$, converge to the asymptotic value as expected since the ratio $a/R_s \Rightarrow 0$. The linear extrapolation shown in figure 4 for the nuclear matter limit gives a good estimate for the nuclear matter surface energy coefficient. It can be seen from the figure that the extrapolated value of a_s for full $H(r)$ and the corresponding semi-infinite approximation differ by about 1·5 MeV. In these surface moment calculations, we have used for the ε_0 the value of energy density h_0 at the centre of the nucleus with mass number A, which is to be associated with the volume energy coefficient inclusive of the compressibility effects. Figure 5 shows the plot of this quantity for the two forces RATP and SIII. For semi-infinite approximation case the plot of the volume term coefficient a_v shows the expected parabolic dependence in $A^{-1/3}$ due to compressibility effects. For full $H(r)$, the volume term shows deviations from this simple parabolic dependence for small mass numbers. The increase in this quantity arises only due to the Δ-terms. For

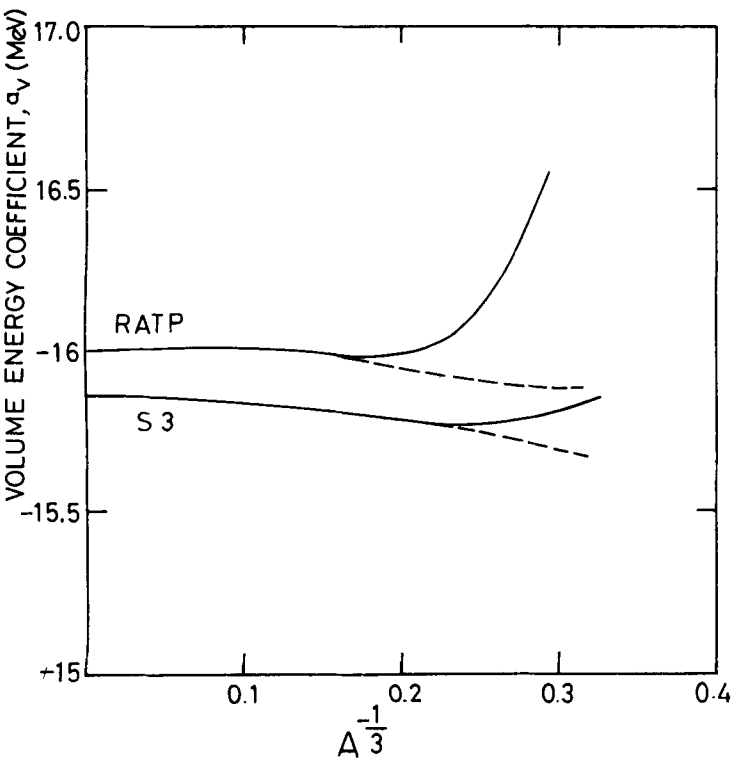

Figure 5. The plot of volume energy coefficient a_v versus $A^{-1/3}$ for SIII and RATP forces. The dashed curve shows the result with semi-infinite approximation in τ expressions.

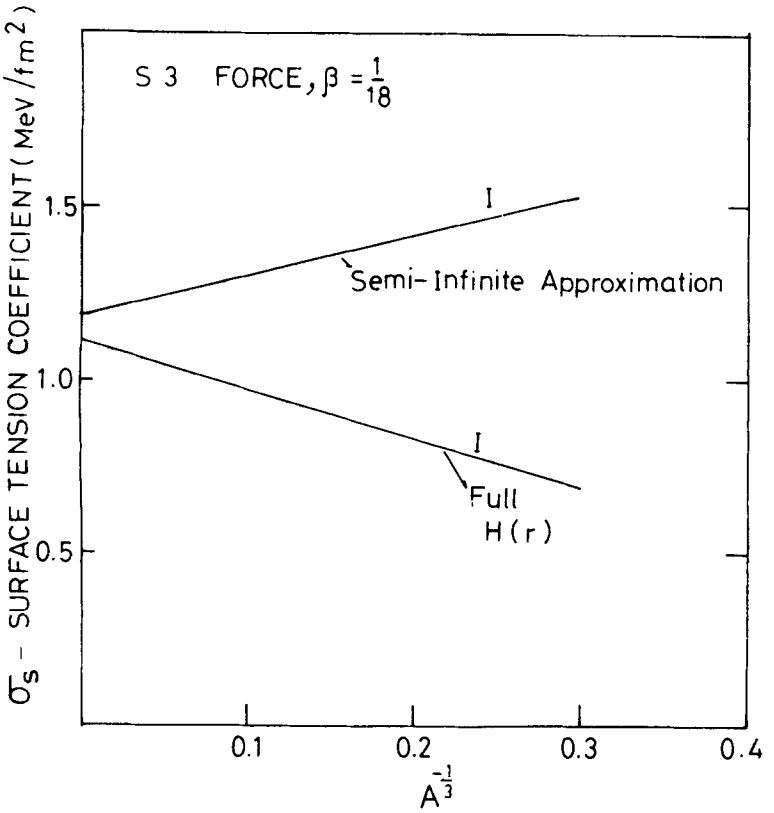

Figure 6. Same as for figure 5, but for surface tension coefficient $\sigma_s(A)$ as a function of $A^{-1/3}$.

RATP force this contribution is rather very large, whereas for SIII and SkM forces these deviations are small and very similar.

The surface tension coefficient σ_s calculated as a coefficient of $4\pi R_s^2$ term in (3) for the total energy density $H(r)$ and is plotted in figure 6 and it almost decreases linearly with $A^{-1/3}$ for SIII force. For semi-infinite approximation $\Delta\rho = \partial^2\rho/\partial r^2$ in the calculation of energy density $H(r)$, the derived surface tension coefficient σ_s increases almost linearly with $A^{-1/3}$. This increase of σ_s with mass number arises due to the diffuseness correction in the sharp cut-off radius R_s. This diffuseness contribution gives rise to geometric contribution from the surface energy term [10] to the curvature energy term.

The effective curvature energy coefficient a_c^* consists of three parts [1, 6, 9] volume compressibility contribution from a_v'' expansion; geometrical component from surface moment expansion of a_s', and the leading term of the curvature moment expansion a_c^∞ as given in (8). The plots of the curvature moments a_c as a function of $A^{-1/3}$ are shown in figure 7 for the full $H(r)$, and for $H(r)$ calculated under the semi-infinite approximation. Table 3 contains the values of a_c^*, and its components obtained by extrapolation of the surface moment a_s, volume term a_v and curvature moment a_c^∞ for the SIII interaction for the two cases shown in the figures 4, 5 and 7. It can be seen from table 3, that the effective a_c^* is smaller in magnitude and even negative for total $H(r)$ density profiles. Whereas, the value of a_c^* for the semi-infinite approximation

Table 3. Three components of effective curvature energy a_c^*, using the surface moments of $H(r)$ around the sharp radius R_s, with and without the semi-infinite approximation in the Δ term in the kinetic energy term $\tau(r)$.

Force	Case	a'_s	a'''_v	a_c^∞	a_c^*
SIII	Total $H(r)$	−25·73	2·44	22·82	−0·5
	Semi-infinite	15·94	2·20	−8·92	9·24

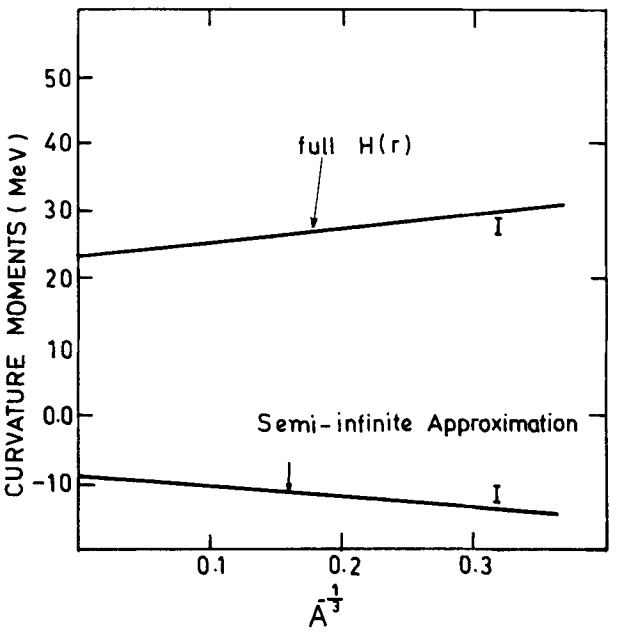

Figure 7. Same as for figure 5, but for curvature moments of $H(r)$.

of $H(r)$ is positive, large $\cong 9$ MeV and is comparable with the values obtained in earlier studies of curvature energies.

The second moments of the surface expansion of $H(r)$ i.e. Gauss curvature moments have been plotted against the $A^{-1/3}$ in figure 8 for SIII forces. It can be seen that for semi-infinite approximation the value of $a_0 \cong 8$ MeV and does not vary much with mass number (variation less than 2 MeV) showing that the shape of the surface peaked integrand does not change with mass number and the accuracy of the surface moments is of the order of 1 MeV. For total $H(r)$, the a_0 values vary from -5 to 8 MeV in the mass range of interest, indicating that in this case the surface structure changes and the second moment brings this out dramatically by changing from negative to positive values. The effective values of a_0^* is a sum of contribution from a_v, a_s, a_c expansions as given in (8).

In order to obtain the surface, curvature energy coefficients for the nuclear matter limit in a more quantitive way, we have used the power series expansions given in eq. (8), and the surface, curvature and gaussian curvature moments calculated for the sequence of nuclei. Table 4 gives these values for the three representative Skyrme parameter sets. The magnitude of curvature energy coefficient in the present

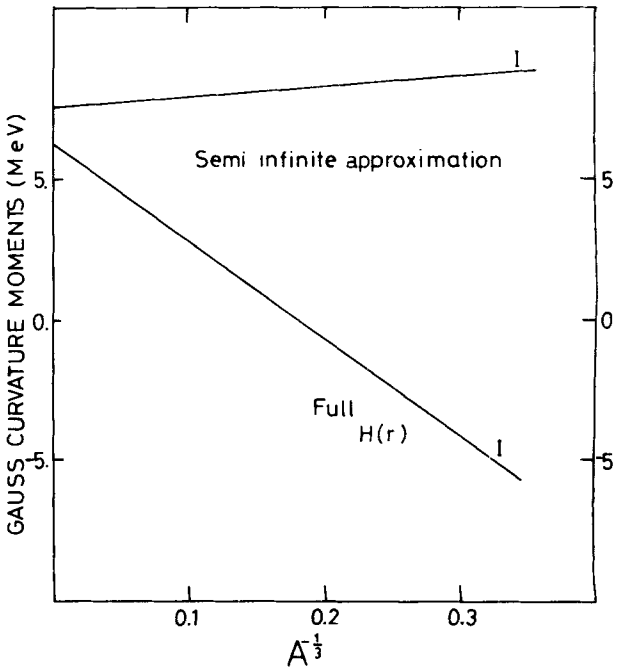

Figure 8. Same as for figure 5, but for Gauss curvature moments of $H(r)$.

Table 4. Nuclear matter values of the volume energy coefficient, surface energy coefficient, effective curvature energy coefficient and Gauss effective energy coefficient for the three Skyrme forces using the total $H(r)$ and the proposed procedure. The second row for each force is obtained by fitting the total energy E_T to the leptodermous expansion of eq. (4).

Force	a_v^∞	a_s^∞	a_c^*	a_0^*
SIII	−15·847	19·26	−0·5	27·0
SIII	—	—	$-1{\cdot}0^+$	$17{\cdot}8^+$
SkM	−15·71	17·92	2·4	21·0
SkM	—	—	$3{\cdot}8^+$	$12{\cdot}0^+$
RATP	−15·96	18·90	3·4	20·0
RATP	—	—	$4{\cdot}8^+$	$12{\cdot}7^+$

calculations is found to be very small, the sign depending on the Skyrme interaction parameters. The values for the a_c^* obtained in the present calculations are very much different from those obtained in earlier studies for all the three Skyrme forces. For some Skyrme forces this term is even negative, whereas all earlier calculations lead to large postive values only.

Another way to obtain the coefficients in the LDM mass relations is to expand the total energy E_T in power series of $A^{-1/3}$ directly as in (4). These fitted constants are highly correlated. However in model masses, one can fix the leading term volume energy a_v^* and surface constant a_s^* depending on the Skyrme interaction chosen, and therefore, one can obtain the remaining curvature terms reliably by fitting directly E_T values. Tables 4, also contains the values (denoted by +) so obtained which are in general agreement with the values deduced from the surface moment expansion, and thus shows the accuracy of the procedure adopted. These calculated coefficients (a_v^*, a_s^*, a_c^*, a_0^*) are consistent with semi-empirical mass fits, which demand small values of a_c^* and non-zero values of a_0^* coefficient.

4. Summary

In conclusion, leptodermous expansion of the ground state energies E_T of finite nuclei has been carried out starting from the semi-classical EDF theory. The surface, curvature and Gauss curvature contributions were obtained from the surface moments of the energy density profile $H(r)$ around sharp cut-off radius R_s for a sequence of nuclei with $N = Z$ and without any Coulomb interaction. A transition to the LDM type expansion in $A^{-1/3}$ was then made by power series expansion of the surface moments of finite nuclei. The effective curvature energy coefficient a_c^* was found to be very small for the three Skyrme forces S-III, SkM, RATP for LDM type expansion. The calculated total energies E_T when fitted by the least squares to eq. (4) also yielded same values for the LDM coefficients as obtained from the leptodermous expansion method and the power series expansion as in eq. (8). It was also found that the semi-infinite approximation as used in earlier EDF calculations results in overestimates of effective curvature energy. Thus we have resolved the anomaly in the curvature energy coefficient calculated on the basis of EDF formalism and its semi-empirical estimate from the least squares fit to the experimental ground state masses.

Acknowledgements

One of the authors (SKK) is thankful to J Treiner and H Krivine and O Bohigas for use of their code in solving the Euler's equation for density profiles and also for many fruitful discussions on various aspects of this problem in the initial stages of this work during his stay at Institut de Physique Nucleaire, Orsay. We are also thankful to S S Kapoor for many suggestions during the course of these studies. We are greatly indebted to the referee for carefully going through the manuscript and making very useful suggestions in making it concise and clear.

References

[1] M Brack, C Guet and H-B Hakansson, *Phys. Rep.* **123**, 275 (1985)
[2] W D Myers and W J Swiatecki, *Ann. Phys.* **55**, 395 (1969)
[3] W D Myers, *Droplet model of atomic nuclei*, (IFI/Plenum, New York, 1977)
[4] P A Seeger and W M Howard, *Nucl. Phys.* **A238**, 491 (1975)
[5] H J Krappe, J R Nix and A J Sierk, *Phys. Rev.* **C22**, 992 (1979)
[6] J Treiner and H Krivine, *Ann. Phys.* **170**, 406 (1986)
[7] J W Negele and D Vautherin, *Nucl. Phys.* **A207**, 298 (1973)

[8] W Stocker, J Bartel, J R Nix and A J Sierk, **A489**, 252 (1988)
M Brack, *Phys. Rev.* **B39**, 3533 (1989)
M Durand, P Schuck and X Vinas, ISN Grenoble Preprint (1991)
[9] B Grammaticos, *Z. Phys.* **A312**, 99 (1983)
[10] S K Kataria, V S Ramamurthy, S S Kapoor, Aruna Nijasure and A K Dutta, *DAE symp. on Nucl. Phys.*, Bombay, **B31**, 3 (1988)
[11] P Hohenberg and W Kohn, *Phys. Rev.* **136**, B864 (1964)
[12] F Tondeur, A K Dutta, J M Pearson and R Behrman, *Nucl. Phys.* **A470**, 93 (1987)